

This discussion paper is/has been under review for the journal *Atmospheric Chemistry and Physics (ACP)*. Please refer to the corresponding final paper in *ACP* if available.

**Influence of
meteorological
variability on
interannual variations**

J. Kurokawa et al.

Influence of meteorological variability on interannual variations of the springtime boundary layer ozone over Japan during 1981–2005

J. Kurokawa¹, T. Ohara¹, I. Uno², M. Hayasaka³, and H. Tanimoto¹

¹National Institute for Environmental Studies, Onogawa, Tsukuba, Ibaraki, Japan

²Research Institute for Applied Mechanics, Kyushu University, Kasuga, Fukuoka, Japan

³Center for Environmental Remote Sensing, Chiba University, Yayoi, Inage, Chiba, Japan

Received: 21 February 2009 – Accepted: 11 March 2009 – Published: 23 March 2009

Correspondence to: J. Kurokawa (kurokawa.junichi@nies.go.jp)

Published by Copernicus Publications on behalf of the European Geosciences Union.

Title Page

Abstract

Introduction

Conclusions

References

Tables

Figures

⏪

⏩

◀

▶

Back

Close

Full Screen / Esc

Printer-friendly Version

Interactive Discussion

Abstract

We investigated the influence of meteorological variability on the interannual variation of the springtime boundary layer ozone over Japan during 1981–2005 by multiyear simulations with the Models-3 Community Multiscale Air Quality (CMAQ) modeling system and the Regional Emission Inventory in Asia (REAS). CMAQ/REAS generally reproduced the observed interannual variability of springtime ozone over Japan, showing year-to-year variations larger than the annual rate of increase of the long-term trend. We then analyzed the influence of the interannual variation of meteorological fields in simulated results by using the fixed emissions for 2000 and meteorology data for each year. As a reference parameter, we calculated the area-weighted surface pressure anomaly over the Pacific Ocean east of Japan. When the anomaly has a large negative value, polluted air masses from continental Asia tend to be transported directly to Japan by westerly winds. In contrast, when the anomaly has a large positive value, the influences of the outflow from continental Asia tends to be small because the westerly components of wind fields around Japan are comparatively weak. Instead, southerly winds are relatively strong and transport clean air masses from the Pacific Ocean to Japan. Consequently, springtime ozone over Japan is higher (lower) than in ordinary years when the anomaly has a large negative (positive) value. In general, the interannual variation of springtime ozone over Japan is sensitive to the outflow from continental Asia. We also found some correlation between springtime ozone over Japan and the El Niño-Southern Oscillation, indicating that higher and lower springtime ozone over Japan are related to La Niña and El Niño, respectively. Differences in the meridional displacement and diversity of cyclone tracks near Japan between El Niño and La Niña years may be responsible for interannual variations in the springtime boundary layer ozone over Japan.

ACPD

9, 7555–7588, 2009

Influence of meteorological variability on interannual variations

J. Kurokawa et al.

Title Page

Abstract

Introduction

Conclusions

References

Tables

Figures

⏪

⏩

◀

▶

Back

Close

Full Screen / Esc

Printer-friendly Version

Interactive Discussion

1 Introduction

Tropospheric ozone (O_3) is a key species in atmospheric chemistry. O_3 and its photochemical derivative OH, are major oxidants of most natural and anthropogenic compounds and play controlling roles in the oxidation capacity of the atmosphere. In addition, tropospheric O_3 has large impacts on the climatological environment as a greenhouse gas (Intergovernmental Panel on Climate Change, 2007) and negatively affects human health, agricultural crops, and natural vegetations (Wang and Mauzerall, 2004; Mauzerall et al., 2005). Therefore, understanding the spatial distribution, long-term trends, and interannual variation (IAV) of tropospheric O_3 is very important.

In Japan, surface and boundary layer (BL) O_3 has increased continuously since the 1980s despite reductions in the concentrations of nitrogen oxides ($NO_x=NO+NO_2$) and non-methane volatile organic compounds (NMVOC), which are precursors of O_3 (Ohara et al., 2008). Many studies have reported that trans-boundary transport of O_3 and its precursors, especially from East Asia, has greatly influenced the recent increase trends of O_3 over Japan (Pochanart et al., 1999; Naja and Akimoto, 2004; Tanimoto et al., 2005; Yamaji et al., 2006, 2008). Tanimoto et al. (2005) estimated that the regional build-up of O_3 due to anthropogenic emissions in eastern China and Korea accounts for about 10 ppbv in March and April and about 20 ppbv in May over Japan. Ohara et al. (2007) reported that emissions of O_3 precursors in Asia, particularly in China, have been growing rapidly during the past two decades. Thus, it is probable that the impacts of trans-boundary pollution are becoming correspondingly larger.

Although O_3 concentrations over Japan show a long-term increasing trend, they also show large year-to-year variations (Ohara et al., 2008). The considerable factors causing these variations are the IAV of O_3 precursor emissions, biomass burning, stratospheric O_3 , and meteorological fields. Although anthropogenic emissions from Japan and other Asian countries such as China and Korea have a large impact on the O_3 concentration over Japan, we have been unable to identify year-to-year variations (in contrast to the long-term trend) in the IAV of these anthropogenic

Influence of meteorological variability on interannual variations

J. Kurokawa et al.

Title Page

Abstract

Introduction

Conclusions

References

Tables

Figures

⏪

⏩

◀

▶

Back

Close

Full Screen / Esc

Printer-friendly Version

Interactive Discussion

Influence of meteorological variability on interannual variations

J. Kurokawa et al.

[Title Page](#)[Abstract](#)[Introduction](#)[Conclusions](#)[References](#)[Tables](#)[Figures](#)[⏪](#)[⏩](#)[◀](#)[▶](#)[Back](#)[Close](#)[Full Screen / Esc](#)[Printer-friendly Version](#)[Interactive Discussion](#)

emissions similar to those in O_3 concentrations over Japan (Ohara et al., 2007, <http://www.jamstec.go.jp/frcgc/research/d4/emission.htm>; Ohara et al., 2008). Several studies have reported that the IAV of wildfire emissions and of the O_3 produced by them is an important factor affecting the IAV of tropospheric O_3 (Doherty et al., 2006; Koumoutsaris et al., 2008). In this study, we did not focus on the effects of year-to-year variations in biomass burning emissions on O_3 over Japan. Recently, the influences of lower stratospheric O_3 and stratosphere-troposphere exchange on the IAV of tropospheric O_3 have been analyzed (Ordóñez et al., 2007; Koumoutsaris et al., 2008; Terao et al., 2008). Terao et al. (2008) indicated that in the northern extratropics such as over Canada and Europe, tropospheric O_3 is highly influenced by O_3 in the lower stratosphere, but stratospheric influences are small in the other regions, especially those influenced by large transports of O_3 from East Asia. With respect to meteorological fields, several studies have reported the influences of the IAV of continental-Asia outflow on the tropospheric O_3 and its relations to El Niño-Southern Oscillation (ENSO) (Liu et al., 2003, 2005; Koumoutsaris et al., 2008). However, the influences of meteorological fields on the IAV of O_3 over the northwestern Pacific region, including Japan, where the impacts of continental-Asia outflow are significantly high, have not been studied.

The purpose of this study was to investigate the effects of meteorological variability on the IAV of O_3 over Japan. It is expected that transport of polluted air masses from continental Asia will continue to increase and these air masses are known to have their greatest effect on the springtime BL (Akimoto, 2003; Zhang et al., 2004; Tanimoto et al., 2005; Yamaji et al., 2006, 2008). Thus, in this work we focused on the influences of the IAV of continental-Asia outflow on the springtime BL O_3 over Japan. We conducted two sets of multiyear springtime simulations during 1981–2005 using the Models-3 Community Multiscale Air Quality (CMAQ) modeling system (Byun and Schere, 2006) and the Regional Emission Inventory in Asia (REAS). First, we evaluated reproducibility of the observed IAV of O_3 over Japan by simulated results using emission data sets and meteorological fields for each year. Then, we examined the influences of the IAV of

meteorological fields and the processes causing the relatively higher and lower spring-time BL O₃ over Japan by simulated results using fixed emissions for 2000. Finally, we discussed the relationships between ENSO events and the IAV of O₃ over Japan. We define several abbreviations in this paper, and provide a list of them in Table 1 for the reader's convenience.

2 Model description

2.1 Chemical transport model

The three-dimensional regional-scale chemical transport model used in this work was developed jointly by Kyushu University and the National Institute for Environmental Studies (NIES) (Uno et al., 2005), based on the Models-3 CMAQ version 4.4 modeling system released by the US Environmental Protection Agency (Byun and Schere, 2006). This model is driven by meteorological fields generated by the Regional Atmospheric Modeling System (RAMS) version 4.4 (Pielke et al., 1992). The horizontal model domain for the CMAQ simulation is 6240×5440 km² on a rotated polar stereographic map projection centered at 25° N, 115° E, with a grid resolution of 80×80 km² (Fig. 1). For vertical resolution, we used 14 layers up to 23 km in the sigma-z coordinate system. In this study, we defined the BL as from the surface to an altitude of 1 km; the BL comprises 5 layers in the model coordinate system. We adopted the Statewide Air Pollution Research Center (SAPRC)-99 scheme (Carter et al., 2000) for gas-phase chemistry (with 72 chemical species and 214 chemical reactions, including 30 photochemical reactions). For aerosol calculations, we applied the third-generation CMAQ aerosol module (AERO3), which includes the Secondary Organic Aerosols Model (SORGAM) (Schell et al., 2001) as a secondary organic aerosol model, ISORROPIA (Nenes et al., 1998) as an inorganic aerosol model, and the piecewise parabolic method (PPM) (Binkowski and Shankar, 1995) as the regional particulate model. Note that both the

Influence of meteorological variability on interannual variations

J. Kurokawa et al.

Title Page

Abstract

Introduction

Conclusions

References

Tables

Figures

⏪

⏩

◀

▶

Back

Close

Full Screen / Esc

Printer-friendly Version

Interactive Discussion

gas-phase chemistry and aerosol schemes are applicable only to the tropospheric atmosphere. Schemes applicable to the stratosphere are not used in the model.

2.2 Outline and setting of the numerical experiments

We conducted two sets of numerical experiments. First, we performed a 25-year springtime simulation for 1981–2005 using emission data sets and meteorological fields for each year (called “ $E_{yy}M_{yy}$ ”). Second, we conducted a simulation for the same period using the fixed emissions for 2000 and the meteorological fields for each year (called “ $E_{00}M_{yy}$ ”). We performed simulations for the period from 1 January to 31 May of each year. In this study, we defined springtime as April and May, and thus treated the first 3 months as the spin-up period. The purpose of $E_{yy}M_{yy}$ was to evaluate the ability of the model to reproduce the observed results. In this work, we focused on the influence of meteorological variability on the IAV of springtime BL O_3 over Japan. Therefore, the simulated $E_{00}M_{yy}$ results, which elucidate the sensitivity of springtime BL O_3 over Japan to meteorological factors, are mainly used in the following analysis.

Both experiments used the same meteorological fields and initial and boundary conditions for chemical tracers. Meteorological fields for each year were generated by RAMS with initial and boundary conditions defined by the National Centers for Environmental Prediction/National Center for Atmospheric Research (NCEP/NCAR) Reanalysis 1 data sets (<http://www.cdc.noaa.gov/cdc/data.ncep.reanalysis.html>) (Kalnay et al., 1996; Kistler et al., 2001). The reanalysis data sets have a spatial resolution of $2.5^\circ \times 2.5^\circ$ and a temporal resolution of 6 h. The initial fields of chemical compounds were prepared by the initial conditions processor (ICON) of the CMAQ modeling system (Byun and Schere, 2006). The influence of the initial condition was eliminated during the spin-up period (3 months). The monthly averaged lateral boundary conditions for most chemical tracers were obtained from the global chemical transport model CHASER (Chemical AGCM for Study of Atmospheric Environment and Radiative Forcing; Sudo et al., 2002). In this study, we did not examine the influences of the IAV of inflow from outside of Asia or stratospheric O_3 . Thus, we assumed no IAV as the lateral

Influence of meteorological variability on interannual variations

J. Kurokawa et al.

Title Page

Abstract

Introduction

Conclusions

References

Tables

Figures

⏪

⏩

◀

▶

Back

Close

Full Screen / Esc

Printer-friendly Version

Interactive Discussion



boundary condition, and we set the inflow concentrations of O₃ from the stratosphere to zero.

$E_{yy}M_{yy}$ requires the emission inventories for 1981–2005, and $E_{00}M_{yy}$ needs only the data set from 2000. We prepared data sets for anthropogenic emissions of sulfur dioxides (SO₂), NO_x, carbon monoxide (CO), NMVOC, black carbon, organic carbon, and ammonia (NH₃) using REAS version 1.1 (Ohara et al., 2007, <http://www.jamstec.go.jp/frcgc/research/p3/emission.htm>). REAS data sets include most anthropogenic sources such as fuel combustion and industrial processes for 1981–2003. We extended the data sets until 2005 using the same methodology as Ohara et al. (2007) and new statistics such as energy consumption and industrial activities (e.g. International Energy Agency, 2006; United Nations, 2005, 2006). We took parameters such as emission factors and removal efficiencies from those for the year 2003. Springtime emission is exactly the same as annual average flux in this study because seasonal variation is not considered in the REAS database. According to Streets et al. (2003), springtime fractions of annual emissions in China are similar to the annual mean value. We took biogenic emissions of isoprene and monoterpenes from monthly estimations for the 1990s by Guenther et al. (1995). We did not include NO_x emissions from soil or lightning in the model. With respect to biomass burning emissions, Koumoutsaris et al. (2008) reported that variations in emission intensity and transports of O₃ produced by them have some impact on the IAV of springtime tropospheric O₃. However, our focus was not on the effects of year-to-year changes in wildfire emissions, and in Asia, their recent long-term trend is smaller than that of anthropogenic emissions. Thus, we used climatological inventories for the late 1990s from Streets et al. (2003) in this work.

The modeling system described above has previously been used for analyzing tropospheric ozone over East Asia including Japan (See Uno et al., 2005; Tanimoto et al., 2005; Yamaji et al., 2006, 2008) and in these studies, the simulated results show good agreement with observations.

Influence of meteorological variability on interannual variations

J. Kurokawa et al.

[Title Page](#)[Abstract](#)[Introduction](#)[Conclusions](#)[References](#)[Tables](#)[Figures](#)[⏪](#)[⏩](#)[◀](#)[▶](#)[Back](#)[Close](#)[Full Screen / Esc](#)[Printer-friendly Version](#)[Interactive Discussion](#)

3 Results and discussions

3.1 The climatological springtime BL O₃ over East Asia

First, we describe the general features of the modeled climatological springtime BL O₃ over East Asia (25-year average during 1981–2005). In this study, we define the simulated springtime BL O₃ as the O₃ concentration averaged over the lower 5 layers of the model (from the surface to 1 km of altitude) during April and May. The spatial distribution of climatological BL O₃, simulated by $E_{yy}M_{yy}$, is shown in Fig. 2a, overlaid with the climatological springtime wind fields in the BL. High O₃ of more than 55 ppbv is widespread over central eastern China (CEC; Fig. 1), the Korean peninsula, and Japan. The mean wind fields in the high O₃ area are westerly and southwesterly, suggesting that polluted air masses of continental Asia are likely to be transported to Japan. O₃ concentrations over the Pacific Ocean south of Japan are generally low.

Figure 2b shows the spatial distribution of climatological springtime BL O₃, as in Fig. 2a, but simulated by $E_{00}M_{yy}$, along with the standard deviation of the O₃ concentration at each grid cell (contours) calculated from the simulated results by $E_{00}M_{yy}$ for each year and the climatological fields. Although the concentrations of O₃ simulated by $E_{00}M_{yy}$ (Fig. 2b) are slightly higher than those simulated by $E_{yy}M_{yy}$ (Fig. 2a), their spatial distributions are very similar. Thus, the use of 2000 as the fixed emission inventory base year for the numerical experiment (i.e. $E_{00}M_{yy}$) is appropriate. The standard deviation maxima are south of the Japanese Islands, where the climatological O₃ gradient is largest and thus, sensitivity to the IAV of O₃ can be considered to be high. Over the Japanese Islands, O₃ variability is largest over western and central Japan (WCJ; defined in Fig. 1), especially in the western part of this region, where influences of O₃ from continental Asia are expected to be large. In contrast, the IAV of O₃ is relatively small in northern Japan. Therefore, in the following sections, we analyze mainly the IAV of the springtime BL O₃ over WCJ.

Influence of meteorological variability on interannual variations

J. Kurokawa et al.

Title Page

Abstract

Introduction

Conclusions

References

Tables

Figures

⏪

⏩

◀

▶

Back

Close

Full Screen / Esc

Printer-friendly Version

Interactive Discussion

3.2 The interannual variation of springtime BL O_3 over western and central Japan

In Japan, continuous measurements of general air pollution are in operation at air quality monitoring stations all around the country. The stations are managed and operated by Ministry of Environment Japan and local governments. At the stations, the mixing ratios of photochemical oxidants (O_x) are observed by absorption spectrophotometry using a neutral potassium iodide solution (KI method) or photometric instruments based on absorption in the ultraviolet region (UV method). The majority (about 70% for the year of 2006) of individual analyzer for O_x measurement was calibrated by KI method at each station. However, variability of the scales obtained from individual KI method seems to be larger than that by UV method. Recently, Ministry of Environment Japan has reported the results of inter-comparison experiments for standards for O_x measurements of 25 local governments using the Standard Reference Photometer (SRP) #35, built by the National Institute of Standard and Technology (NIST) and maintained by NIES (Mukai et al., 2007). According to this report, the variability of KI method and UV method was, respectively about 5.6% and 1.1% as one standard deviation. Also KI scale for O_x showed about 9% larger sensitivity than O_3 scale. However, in this study, O_x observations are used for evaluation of the year-to-year variations of O_3 over WCJ. In addition, there are no other data sets which have long-term observation records all over WCJ. For these reasons, we used the observation data at 136 air quality monitoring stations in WCJ, where O_x was measured continuously during 1985–2005. The stations selected here are located in urban, suburban, and rural areas and at altitudes blow 1 km above mean sea level.

Figure 3a compares the time series of observed springtime surface O_x anomalies averaged over WCJ with those of the springtime BL O_3 simulated by $E_{yy}M_{yy}$ for 1985–2005. For the calculation of the springtime mean and standard deviation of observed O_x over WCJ, we first calculate the springtime-averaged value for each station using data from all hours of the day. Then, we calculate the mean and standard deviation from the station averages with equal weight. Note that the anomalies used in this

Influence of meteorological variability on interannual variations

J. Kurokawa et al.

Title Page

Abstract

Introduction

Conclusions

References

Tables

Figures

⏪

⏩

◀

▶

Back

Close

Full Screen / Esc

Printer-friendly Version

Interactive Discussion

Influence of meteorological variability on interannual variations

J. Kurokawa et al.

Title Page

Abstract

Introduction

Conclusions

References

Tables

Figures

⏪

⏩

◀

▶

Back

Close

Full Screen / Esc

Printer-friendly Version

Interactive Discussion

section for the comparison of observed and simulated results are defined as deviations from the values averaged over 1985–2005, although period of model simulation is from 1981 to 2005. Both observed (blue points) and simulated (black line) results show larger year-to-year variations than the annual rate of increase of the long-term trend. CMAQ reproduced the observed local minima in 1986, 1995, and 1998 and the local maxima in 1996 and 1999–2000. Observed anomalies decreased from 1996 to 1998 and from 2000 to 2002, in contrast to the long-term trend, and these features were also well reproduced by CMAQ. The amplitude of the IAV during 1987 and 1991 was relatively small in both observed and simulated results. Simulated anomalies show a large increase from 1991 to 1992 and a decrease from 2002 to 2003, neither of which is found in the observation data. However, CMAQ generally reproduced well the observed IAV of springtime surface O_3 anomalies over WCJ. We also compared the IAV of springtime BL O_3 anomalies simulated by $E_{yy}M_{yy}$ (black line) with that simulated by $E_{00}M_{yy}$ (red line; Fig. 3). In both scenarios, the IAV of O_3 anomalies shows clearly similar patterns, especially the large year-to-year variations. As described in Sect. 2.2, the $E_{00}M_{yy}$ scenario uses the fixed emissions for 2000 and the meteorological fields for each year. Therefore, these results suggest that the short-term IAV of springtime surface and BL O_3 over WCJ is determined mainly by the meteorological variability.

Figure 3b compares the time series of springtime surface mixing ratios of observed O_x and simulated O_3 for the $E_{yy}M_{yy}$ scenario averaged over WCJ during 1985–2005. Simulated surface O_3 mixing ratios are generally about 20 ppbv larger than observed O_x . One possible reason of this discrepancy is relatively coarse horizontal and vertical resolutions of the model grids. These might cause the underestimation of NO_x titration of O_3 , especially in urban and suburban areas. However, our focus is on the year-to-year variations of O_3 over WCJ and especially the influences of meteorological variability on them. Thus, we consider that this discrepancy of absolute concentration is not an essential problem for this study. Note that both observed and simulated results show clear and significant (at 99% significance level) increasing trends in Fig. 3b, with respective rate of increase of about 0.37 and 0.40 [ppbv/year]. No such long-term

trend is found in the results simulate by $E_{00}M_{yy}$ (Fig. 3a), which suggests that the increase in the observed anomalies was caused by the recent increase of anthropogenic emissions in East Asia (Ohara et al., 2008).

3.3 Years of high and low springtime BL O_3 over western and central Japan

5 In some years, the springtime BL O_3 over WCJ simulated by $E_{00}M_{yy}$ is much higher or lower than in other years, even though the same emission data set was used (Fig. 3). To analyze these features, in this section we define “high (low) O_3 over WCJ years” as the top (bottom) 5 years between 1981 and 2005 with respect to the springtime BL O_3 anomalies simulated by $E_{00}M_{yy}$. The high O_3 over WCJ years are 1992, 1996,
10 1999, 2000, and 2005. The low O_3 over WCJ years are 1983, 1986, 1991, 1998, and 2003. Figure 4 shows the composite springtime BL O_3 fields (a and b), its anomalies (c and d), and springtime surface pressure anomalies (e and f) for the high (a, c, and e) and low (b, d, and f) O_3 over WCJ years. The overlaid vectors in Fig. 4a and b are the composite springtime wind fields in the BL, and those in Fig. 4c, d, e, and f are the composite wind field anomalies. Note that in this and the following sections, all analyses are based on the results simulated by $E_{00}M_{yy}$ and anomalies are redefined as the deviations from values averaged over 1981–2005.

First, we describe the general features of the composite field of high O_3 over WCJ years. The area of high O_3 over CEC, the Korean peninsula, and Japan (Fig. 4a) is slightly larger and shifted southward compared with the climatological field (Fig. 2b). Correspondingly, high positive O_3 anomalies are widespread over the area south of the high O_3 from the eastern coast of China to south of the Japanese Islands (Fig. 4c). WCJ is near the center of the high O_3 area and on the edge of the high positive anomaly region. Mean wind fields (Fig. 4a) and the mean wind field anomalies (Fig. 4c and e)
25 over WCJ show that westerly components are stronger and southerly components are weaker than in the climatological wind fields. This suggests that in high O_3 over WCJ years, WCJ is strongly influenced by continental-Asia outflow but less influenced by maritime air masses from the Pacific Ocean. The northeastern area, including north-

Influence of meteorological variability on interannual variations

J. Kurokawa et al.

Title Page

Abstract

Introduction

Conclusions

References

Tables

Figures

◀

▶

◀

▶

Back

Close

Full Screen / Esc

Printer-friendly Version

Interactive Discussion



Influence of meteorological variability on interannual variations

J. Kurokawa et al.

[Title Page](#)[Abstract](#)[Introduction](#)[Conclusions](#)[References](#)[Tables](#)[Figures](#)[Back](#)[Close](#)[Full Screen / Esc](#)[Printer-friendly Version](#)[Interactive Discussion](#)

ern Japan, is outside the high O_3 area, and weak negative anomalies of O_3 are found there. The westerly component of the wind fields in this area is weaker than the average, which suggests relatively small influences of continental-Asia air masses. With respect to the surface pressure anomalies, negative values are widespread around the Japanese Islands and, especially, over the Pacific Ocean east of Japan (Fig. 4e).

With respect to the low O_3 over WCJ years, the high O_3 area is somewhat smaller and shifted northward (Fig. 4b) compared with in the climatological field (Fig. 2b). WCJ is not near the center of the high O_3 area. The area of negative O_3 anomalies (Fig. 4d) almost coincides with the positive anomaly region in the high O_3 over WCJ years (Fig. 4c). WCJ is on the edge of the negative anomaly region. The mean wind fields (Fig. 4b) and its anomalies (Fig. 4d and f) display weaker westerly components and stronger southerly components over WCJ compared with the climatological field. Thus, these results suggest that in low O_3 over WCJ years, the influence of the continental-Asia outflow on WCJ is smaller and that of maritime air masses from the Pacific Ocean is larger than during ordinary years. The positive O_3 anomalies over the northeastern region might reflect relatively stronger westerly winds, but the values are small. In contrast to the high O_3 over WCJ years, surface pressure anomalies are positive (Fig. 4f). However, the positive anomalies appear in the almost same area as the negative anomalies shown in Fig. 4e.

Finally, on the basis of the above findings, we inferred the processes controlling the springtime BL O_3 concentrations over WCJ as follows:

1. High O_3 over WCJ years

Polluted air masses from continental Asia tend to be transported directly to WCJ by the strong westerly component of the wind field. Meanwhile, the inflow of clean maritime air masses from the Pacific Ocean to WCJ is small because southerly winds around WCJ are weak. As a result, the springtime BL O_3 concentrations over WCJ are higher than during ordinary years. Large negative surface pressure anomalies are present over the Pacific Ocean east of Japan.

Influence of meteorological variability on interannual variations

J. Kurokawa et al.

Title Page

Abstract

Introduction

Conclusions

References

Tables

Figures

◀

▶

◀

▶

Back

Close

Full Screen / Esc

Printer-friendly Version

Interactive Discussion

2. Low O₃ over WCJ years

The influence of the continental-Asia outflow tends to be small because the westerly component of the wind fields around WCJ is relatively weak. On the other hand, southerly winds around WCJ are comparatively strong, and efficiently transport clean air masses from the Pacific Ocean to WCJ. Consequently, the springtime BL O₃ concentration over WCJ is lower than that during an average year. Large positive surface pressure anomalies are present over the Pacific Ocean east of Japan.

It is interesting that large negative and positive surface pressure anomalies, respectively occur in almost the same region during high and low O₃ over WCJ years (Fig. 4e and f, respectively). Thus, as a reference parameter, we calculated the area-weighted surface pressure anomaly (ASPA) in the springtime over the region within the following coordinates (white box in Fig. 4e and f): 141.62° E, 29.31° N; 149.85° E, 27.49° N; 146.82° E, 44.36° N; and 156.02° E, 41.76° N. We then hypothesized that when the ASPA value is negative (positive), O₃ over WCJ should be higher (lower) than during an ordinary year. We examine this hypothesis in the following sections.

3.4 Relationships among springtime BL O₃ over western and central Japan, continental-Asia outflow, and surface pressure anomaly

Time series of springtime ASPA and BL O₃ anomalies over WCJ during 1981–2005 are shown in Fig. 5a. In general, they are negatively correlated especially when the absolute value of ASPA is large such as in 1998 and 2000. On the other hand, no clear relation is observed when the value of ASPA is small such as during the late 1980s. Figure 5b shows a scatter plot and regression lines between springtime ASPA and BL O₃ anomalies over WCJ. The regression lines both for all data and for large ASPA data (larger than 1 hPa) have similar negative slopes. However, as expected, the correlation coefficient ($r = -0.85$) for large ASPA data has a larger negative value than that for all data ($r = -0.79$). These results suggest that ASPA is a good reference parameter for

springtime BL O_3 over WCJ, especially when the absolute value of ASAP is large.

To investigate the relationships among the IAV of O_3 over WCJ, inflow O_3 fluxes to WCJ, and ASPA, we calculated the anomalies of springtime BL O_3 fluxes along sections at the western and southern boundaries of WCJ (L_{WJ} and L_{SJ} , respectively; see Fig. 1). A large O_3 flux anomaly along L_{WJ} (FA_{WJ}) means that the influence of the continental-Asia outflow, which transports high O_3 air masses to WCJ, is large. In contrast, when the O_3 flux anomaly along L_{SJ} (FA_{SJ}) is large, low O_3 air masses are transported to WCJ from the Pacific Ocean. Figure 6a and b display the time series of O_3 anomalies over WCJ and FA_{WJ} and FA_{SJ} , respectively, with the right-hand panels showing the corresponding scatter diagrams and regression lines. Values of FA_{WJ} and FA_{SJ} are normalized relative to the respective 25-year average.

FA_{WJ} and O_3 anomalies over WCJ are generally positively correlated ($r=0.61$); both the correlation coefficient ($r=0.78$) and the slope of regression line for large ASPA data are larger than those for all data. On the other hand, FA_{SJ} and O_3 anomalies over WCJ are negatively correlated ($r=-0.49$). Similar to FA_{WJ} , both r (-0.58) and the slope of the regression line are slightly larger for large ASPA data. We also examined the relations between ASPA and FA_{WJ} and between ASPA and FA_{SJ} . As expected, FA_{WJ} and FA_{SJ} are, respectively negatively and positively correlated with ASPA. For FA_{WJ} r (all data, large ASPA data) is (-0.65 , -0.78) and for FA_{SJ} r is (0.39 , 0.48). These results indicate that when the transport of O_3 from continental Asia is large, that from the Pacific Ocean tends to be small and vice versa, especially when the absolute value of ASPA is large. The IAV of O_3 over WCJ is affected by transport of both high- O_3 air masses from continental Asia and clean maritime air from the south to WCJ. The correlation of O_3 over WCJ with FA_{WJ} is stronger than that with FA_{SJ} , which suggests that the IAV of springtime BL O_3 over WCJ is more sensitive to the continental-Asia outflow. However, there are some years when the maritime air masses have a larger effect. The O_3 anomalies over WCJ in 1997 are smaller than those in 1996 even though FA_{WJ} in 1997 is larger. This is because FA_{SJ} in 1996 was much smaller than in 1997.

We also investigated the IAV of springtime BL O_3 over CEC (region as defined in

Influence of meteorological variability on interannual variations

J. Kurokawa et al.

Title Page

Abstract

Introduction

Conclusions

References

Tables

Figures

⏪

⏩

◀

▶

Back

Close

Full Screen / Esc

Printer-friendly Version

Interactive Discussion

Influence of meteorological variability on interannual variations

J. Kurokawa et al.

[Title Page](#)[Abstract](#)[Introduction](#)[Conclusions](#)[References](#)[Tables](#)[Figures](#)[⏪](#)[⏩](#)[◀](#)[▶](#)[Back](#)[Close](#)[Full Screen / Esc](#)[Printer-friendly Version](#)[Interactive Discussion](#)

Fig. 1). Figure 7a shows the IAV of O_3 anomalies over CEC and ASPA between 1981 and 2005. In general, they are negatively correlated ($r=-0.65$ and -0.71 for all data and large ASPA data, respectively). The wind field anomalies (Fig. 4) suggest that when ASPA has a large positive value (i.e. low O_3 over WCJ years; see Sect. 3.3 and Fig. 4d), relatively strong southerly winds around the southern boundary of CEC (L_{SC} , see Fig. 1) transport lower O_3 air from southern China. In contrast, when ASPA has a large negative value (i.e. high O_3 over WCJ years; see Sect. 3.3 and Fig. 4c), O_3 over CEC tends to be higher because the southerly component of winds around L_{SC} is comparatively weak. We examined these inferences by plotting the time series of O_3 anomalies over CEC and O_3 flux anomalies along section L_{SC} (FA_{SC}) in the springtime BL (Fig. 7b). As expected, the O_3 anomalies and FA_{SC} are negatively correlated ($r=-0.57$ and -0.61 for all data and large ASPA data, respectively). These results indicate that O_3 over CEC is also affected by the IAV of meteorological fields, and they are consistent with the results of He et al. (2008). In addition, springtime BL O_3 over CEC and WCJ are positively correlated ($r=0.61$ and 0.78 for all data and large ASPA data, respectively). Our examination of the relations between FA_{WJ} and springtime westerly winds in the BL averaged over L_{WJ} showed that the correlation coefficients are almost 1, even when all data are included. This finding indicates that the IAV of FA_{WJ} is determined mostly by the IAV of westerly winds over L_{WJ} . However, the recent growth of anthropogenic emissions of O_3 precursors in China might strengthen the influence of O_3 over CEC on the IAV of O_3 over WCJ. This will be examined in a future study.

The above discussion showed that the processes that control the IAV of springtime BL O_3 over WCJ are basically explained by the hypothesis described in Sect. 3.3 (1) and (2), particularly when the absolute value of ASPA is large. However, there are exceptions. The O_3 anomalies over WCJ in 1987 and 1997 were almost average (i.e., zero), although the absolute values of ASPA in these years were larger than 1 hPa. In these years, the region of large O_3 anomalies slightly shifted compared with the composite field (not shown). Moreover, the O_3 anomalies in 1986, 1991, and 1999 were relatively large although the ASPA values of these years were small. The large

surface pressure anomalies in these years were also distributed in slightly different region from the area used to define ASPA (not shown). In these years, we believe that the processes affecting the distribution of O₃ and their relation to meteorological fields were more complicated.

5 3.5 Relation between springtime BL O₃ over western and central Japan and ENSO

Recently, several studies have reported on the relation between the IAV of Asian pollution transport and meteorological variations caused by ENSO and their influences on tropospheric O₃ (Liu et al., 2003, 2005; Koumoutsaris et al., 2008). However, the impacts of ENSO events on the IAV of the O₃ distribution over the northwest Pacific region, including Japan, have not been studied. In this section, we discuss the relation between the IAV of springtime BL O₃ over WCJ and ENSO.

Figure 8 shows the time series of ASPA, O₃ anomalies over WCJ, and the NINO3 index during 1981–2005. NINO3 is the sea surface temperature averaged across the region 5° N–5° S, 150–90° W, expressed as monthly anomalies relative to the 1971–2000 means. We obtained these data from <http://www.cpc.noaa.gov/data/indices> (accessed 20 February 2009). In this study, we used values averaged during November and December of the previous year, considering the response time of continental-Asia outflow to ENSO events, after Koumoutsaris et al. (2008). In general, we found positive correlations between NINO3 and ASPA, and negative correlations between NINO3 and O₃ anomalies. We examined these relationships separately for all data and large ASPA data, as in Sect. 3.4. The correlation coefficients for (all data, large ASPA data) between NINO3 and ASPA and between NINO3 and O₃ anomalies were (0.52, 0.58) and (–0.40, –0.57), respectively. Both relationships are relatively strong when values of ASPA are large, as expected from the results of Sect. 3.4. This result suggests that the high and low O₃ over WCJ years are, respectively related to La Niña (NINO3 is small) and El Niño (NINO3 is large).

Figure 9 displays the mean sea level pressure (MSLP) and cyclone tracks during April and May 1998 and 2000, according to the Japanese 25-year Reanalysis data

Influence of meteorological variability on interannual variations

J. Kurokawa et al.

Title Page

Abstract

Introduction

Conclusions

References

Tables

Figures



Back

Close

Full Screen / Esc

Printer-friendly Version

Interactive Discussion



set (JRA-25; Onogi et al., 2007) produced by the Japan Meteorological Agency and the Central Research Institute of the Electric Power Industry. The cyclone detection and tracking algorithm is based on that used by Serreze (1995) and Serreze et al. (1997), except it has been slightly modified for application to the JRA-25 data set. The MSLP data set was interpolated from $1.25^\circ \times 1.25^\circ$ latitude/longitude grid to the Equal Area Scalable Earth grid over the Northern Hemisphere with a 125-km grid interval. A cyclone center is identified by a local minimum of the interpolated MSLP value. The threshold value of MSLP differences is 0.5 hPa.

We chose the years 1998 and 2000 because they were an El Niño year and a La Niña year, respectively, and because lower (1998) and higher (2000) springtime BL O_3 concentrations over WCJ were seen in both observed and simulated results (Fig. 3). In 1998, a significantly large-scale high-MSLP region, centered at 150° – 170° W, appeared over the whole Pacific. In contrast, the corresponding high-MSLP area in 2000 is smaller than that in 1998 and distributed mainly over the eastern Pacific. Therefore, in 2000, MSLP over the western Pacific, including Japan, was much lower than that in 1998. We expected these differences to appear as lower and higher ASPA, as defined in this study (see Sect. 3.3 and white boxes in Fig. 4e and f). The distribution of cyclone tracks around Japan was clearly different between 1998 and 2000. Two major cyclone tracks over East Asia and the northwestern Pacific in 1998 can be identified: (1) southwest–northeast–oriented course, from the southern coast of the Japanese Islands to the northern Pacific, and (2) a zonally oriented course along 45° – 55° N. On the other hand, cyclone tracks in 2000 show meridional diversity near the Japanese Islands. Some cyclones originated in southeast China or the East China Sea and traveled eastward and northward via the Korean Peninsula, Japan Sea, and the Japanese Islands. This route reflects the preferred meteorological conditions for the transport of continental-Asia air masses to Japan. Consequently, meridional displacement or diversity of cyclone tracks may have caused low (high) O_3 over WCJ in 1998 (2000). Similar features in MSLP fields and cyclone tracks were also found in 1983 (El Niño) and 1985 and 1996 (La Niña) (not shown). In these years, the relationships among MSLP over

Influence of meteorological variability on interannual variations

J. Kurokawa et al.

[Title Page](#)[Abstract](#)[Introduction](#)[Conclusions](#)[References](#)[Tables](#)[Figures](#)[Back](#)[Close](#)[Full Screen / Esc](#)[Printer-friendly Version](#)[Interactive Discussion](#)

the Pacific, continental-Asia outflow, and O_3 concentrations seem to be consistent with the processes controlling springtime BL O_3 over WCJ as described in Sects. 3.3 and 3.4.

The above discussion suggests that it is probable that the meteorological variability caused by the ENSO events is one of the important factors affecting the IAV of springtime BL O_3 over WCJ. However, the timing, period, and intensity of El Niño and La Niña are uncertain; thus, their influences are expected to be complicated. For example, large O_3 anomalies region in 1987 (an El Niño year) slightly shifted compared with the composite field of low O_3 over WCJ years, and ASPA was relatively small in 1989 (a La Niña year). In 1992, despite being an El Niño year, MSLP over the whole Pacific region was exceptionally small; thus, ASPA had a large negative value. The reasons for these discrepancies are not clear, and further studies are needed to understand the relations between ENSO and the IAV of O_3 over WCJ.

4 Conclusions

We investigated the effects of meteorological variability on the interannual variation (IAV) of springtime BL O_3 over Japan. We conducted multiyear springtime simulations during 1981–2005 using the regional scale chemical transport model, CMAQ, and emission inventories, REAS. We performed two sets of numerical experiments. Simulation $E_{yy}M_{yy}$ used the emission data sets and meteorological fields for each year. Another simulation, $E_{00}M_{yy}$ used the fixed emissions for 2000 and meteorological fields for each year. We evaluated the reproducibility of the observed IAV of O_3 over western and central Japan (WCJ) with the modeled results of $E_{yy}M_{yy}$. Then, we analyzed the influences of the IAV of meteorological fields on springtime BL O_3 over WCJ using the simulated results of $E_{00}M_{yy}$. We also examined the relations between ENSO events and the IAV of O_3 over WCJ.

The main results are summarized as follows:

1. The model simulation reproduced well both the short-term variability and the long-

Influence of meteorological variability on interannual variations

J. Kurokawa et al.

Title Page

Abstract

Introduction

Conclusions

References

Tables

Figures



Back

Close

Full Screen / Esc

Printer-friendly Version

Interactive Discussion



Influence of meteorological variability on interannual variations

J. Kurokawa et al.

Title Page

Abstract

Introduction

Conclusions

References

Tables

Figures



Back

Close

Full Screen / Esc

Printer-friendly Version

Interactive Discussion



term trend of the observed springtime surface O_3 over WCJ. Year-to-year variations were larger than the annual rate of increase of the long-term trend. The IAV patterns of O_3 anomalies over WCJ in the simulated results of $E_{yy}M_{yy}$ and $E_{00}M_{yy}$ were clearly similar, suggesting that the IAV of springtime BL O_3 over WCJ is mainly determined by the meteorological variability.

2. The composite O_3 field for the high O_3 over WCJ years showed that a high O_3 area over CEC, the Korean peninsula, and Japan was slightly larger and shifted southward compared with the 25-year-averaged field. On the other hand, the corresponding area for the low O_3 over WCJ years was somewhat smaller and shifted northward. As a result, large O_3 anomalies appeared over WCJ.
3. Large negative (positive) surface pressure anomalies appeared over the Pacific Ocean east of Japan in the composite field of the high (low) O_3 over WCJ years. The area-weighted surface pressure anomaly in the springtime over that region (ASPA) was calculated as a reference parameter. When the absolute value of ASPA was large, ASPA showed good correlation with the IAV of O_3 over WCJ. The IAV of O_3 over WCJ and O_3 flux anomalies along the western and southern boundaries of WCJ also showed good correlation.
4. The processes controlling the IAV of springtime BL O_3 over WCJ can be basically explained as follows. When ASPA has a large negative value, polluted air masses from continental Asia tend to be transported directly to WCJ by the strong westerly component of the wind field. In addition, the inflow of the clean maritime air masses from the Pacific Ocean to WCJ is small because southerly winds are weak. When ASPA has a large positive value, the influence of the continental-Asia outflow tends to be small because the westerly component of the wind fields around WCJ is relatively weak. In contrast, southerly winds around WCJ are relatively strong and transport clean air masses from the Pacific Ocean to WCJ. Consequently, springtime BL O_3 over WCJ is higher (lower) than in ordinary years

Influence of meteorological variability on interannual variations

J. Kurokawa et al.

Title Page

Abstract

Introduction

Conclusions

References

Tables

Figures

◀

▶

◀

▶

Back

Close

Full Screen / Esc

Printer-friendly Version

Interactive Discussion



when ASPA has a large negative (positive) value. In general, the IAV of O_3 over WCJ is sensitive to the continental-Asia outflow.

5. Springtime BL O_3 over WCJ and ENSO events show some correlation and suggest that high and low O_3 over WCJ years are, respectively related to La Niña and El Niño. A massive anticyclone centered in the eastern Pacific appeared in 1998 (El Niño), whereas the maximum MSLP in 2000 (La Niña) was remarkably weak. Meridional displacement or diversity of cyclone tracks near Japan might have influenced the conditions for the transport of continental-Asia air and caused low (high) O_3 over WCJ in 1998 (2000). It is suggested that the meteorological variability caused by ENSO events is one of the important factors affecting the IAV of springtime BL O_3 over WCJ. However, the relation between ENSO and the IAV of O_3 over Japan is complicated and further study is required.

Acknowledgements. This work was supported by the Global Environment Research Fund of the Ministry of the Environment, Japan (C-81). We would like to acknowledge all the staff of air quality monitoring stations of Ministry of Environmental Japan and local governments for carrying out measurements and providing observation data sets. We also would like to thank H. Mukai of NIES for valuable comments. The GFD-DENNOU library, GTOOL, and Generic Mapping Tools (GMT, Wessel and Smith, 1998) were used for drawing the figures.

References

- Akimoto, H.: Global air quality and pollution, *Science*, 302, 1716–1719, 2003.
- Binkowski, F. S. and Shankar, U.: The regional particulate matter model 1. Model description and preliminary results, *J. Geophys. Res.*, 100(D12), 26191–26209, 1995.
- Byun, D. W. and Schere, K. L.: Review of the governing equations, computational algorithms, and other components of the Models-3 Community Multiscale Air Quality (CMAQ) modeling system, *Appl. Mech. Rev.*, 59, 51–77, 2006.
- Carter, W. P. L.: Documentation of the SAPRAC-99 chemical mechanism for VOC reactivity assessment, final report to California Air Resource Board, Contract 92-329 and 95-308, California Air Resource Board, Sacramento, 2000.

Influence of meteorological variability on interannual variationsJ. Kurokawa et al.

[Title Page](#)[Abstract](#)[Introduction](#)[Conclusions](#)[References](#)[Tables](#)[Figures](#)[⏪](#)[⏩](#)[◀](#)[▶](#)[Back](#)[Close](#)[Full Screen / Esc](#)[Printer-friendly Version](#)[Interactive Discussion](#)

Doherty, R. M., Stevenson, D. S., Johnson, C. E., Collins, W. J., and Sanderson, M. G.: Tropospheric ozone and El Niño-Southern Oscillation: Influence of atmospheric dynamics, biomass burning emissions, and future climate change, *J. Geophys. Res.*, 111, D19304, doi:10.1029/2005JD006849, 2006.

5 Guenther, A., Hewitt, C. N., Erickson, D., Fall, R., Geron, C., Graedel, T., Harley, P., Klinger, L., Lerdau, M., McKay, W. A., Pierce, T., Scholes, B., Steinbrecher, R., Tallamraju, R., Taylor, J., and Zimmerman, P.: A global model of natural volatile organic compound emissions, *J. Geophys. Res.*, 100(D5), 8873–8892, 1995.

10 He, Y. J., Uno, I., Wang, Z. F., Pochanart, P., Li, J., and Akimoto, H.: Significant impact of the East Asia monsoon on ozone seasonal behavior in the boundary layer of Eastern China and the west Pacific region, *Atmos. Chem. Phys.*, 8, 7543–7555, 2008, <http://www.atmos-chem-phys.net/8/7543/2008/>.

15 Intergovernmental Panel on Climate Change: Climate Change 2007: The Physical Science Basis: Contribution of Working Group I to the Fourth Assessment Report of the Intergovernmental Panel on Climate Change, edited by: Solomon, S., Qin, D., Manning, M., et al., Cambridge Univ. Press, New York, 2007.

International Energy Agency: Energy Balances of OCED Countries and Energy Balances of Non-OECD Countries [CD-ROM], Paris, 2007.

20 Kalnay, E., Kanamitsu, M., Kistler, R., Collins, W., Deaven, D., Gandin, L., Iredell, M., Saha, S., White, G., Woollen, J., Zhu, Y., Leetmaa, A., Reynolds, R., Chelliah, M., Ebisuzaki, W., Higgins, W., Janowiak, J., Mo, K. C., Ropelewski, C., Wang, J., Jenne, R., and Joseph, D.: The NCEP/NCAR 40-year reanalysis project, *Bull. Amer. Meteorol. Soc.*, 77, 437–471, 1996.

25 Kistler, R., Kalnay, E., Collins, W., Saha, S., White, G., Woollen, J., Chelliah, M., Ebisuzaki, W., Kanamitsu, M., Kousky, V., van den Dool, H., Jenne, R., and Fiorino, M.: The NCEP-NCAR 50-year reanalysis: Monthly means CD-ROM and documentation, *Bull. Amer. Meteorol. Soc.*, 82, 247–267, 2001.

Koumoutsaris, S., Bey, I., Generoso, S., and Thouret, V.: Influence of El Niño-Southern Oscillation on the interannual variability of tropospheric ozone in the northern midlatitudes, *J. Geophys. Res.*, 113, D19301, doi:10.1029/2007JD009753, 2008.

30 Liu, H., Jacob, D. J., Bey, I., Yantosca, R. M., Duncan, B. N., and Sachse, G. W.: Transport pathways for Asian pollution outflow over the Pacific: Interannual and seasonal variations, *J. Geophys. Res.*, 108(D20), 8786, doi:10.1029/2002JD003102, 2003.

Liu, J., Mauzerall, D. L., and Horowitz, L. W.: Analysis of seasonal and interannual variability in

Influence of meteorological variability on interannual variations

J. Kurokawa et al.

[Title Page](#)[Abstract](#)[Introduction](#)[Conclusions](#)[References](#)[Tables](#)[Figures](#)[⏪](#)[⏩](#)[◀](#)[▶](#)[Back](#)[Close](#)[Full Screen / Esc](#)[Printer-friendly Version](#)[Interactive Discussion](#)

- transpacific transport, *J. Geophys. Res.*, 110, D04302, doi:10.1029/2004JD005207, 2005.
- Mauzerall, D. L., Sultan, B., Kim, N., and Bradford, D. F.: NO_x emissions from large point sources: variability in ozone production, resulting health damages and economic costs, *Atmos. Environ.*, 39, 2851–2866, 2005.
- 5 Mukai, H., Hashimoto, S., and Tanimoto, H.: Standards for ozone and green house gases monitoring in Japan (in Japanese), *Proceedings of the 48th Annual Meeting of Japan Society for Atmospheric Environment*, 208–211, 2007.
- Naja, M. and Akimoto, H.: Contribution of regional pollution and long-range transport to the Asia-Pacific region: Analysis of long-term ozonesonde data over Japan, *J. Geophys. Res.*, 109, D21306, doi:10.1029/2004JD004687, 2004.
- 10 Nenes, A., Pandis, S. N., and Pilinis, C.: ISORROPIA: A new thermodynamic equilibrium model for multiphase multicomponent inorganic aerosols, *Aquat. Geochem.*, 4, 123–152, 1998.
- Ohara, T., Akimoto, H., Kurokawa, J., Horii, N., Yamaji, K., Yan, X., and Hayasaka, T.: An Asian emission inventory of anthropogenic emission sources for the period 1980–2020, *Atmos. Chem. Phys.*, 7, 4419–4444, 2007, <http://www.atmos-chem-phys.net/7/4419/2007/>.
- 15 Ohara, T., Yamaji, K., Uno, I., Tanimoto, H., Sugata, S., Nagashima, T., Kurokawa, J., Horii, N., and Akimoto, H.: Long-term simulations of surface ozone in East Asia during 1980–2020 with CMAQ and REAS, edited by Borrego, C. and Miranda, A. I., *NATO Science for peace and security series – C: Environmental Security, Air Pollution Modeling and its Application XIX*, 136–144, ISBN: 978-1-4020-8452-2, Springer, 2008.
- 20 Onogi, K., Tsutsui, J., Koide, H., Sakamoto, M., Kobayashi, S., Hatushika, H., Matsumoto, T., Yamazaki, N., Kamahori, H., Takahashi, K., Kadokura, S., Wada, K., Kato, K., Oyama, R., Ose, T., Mannoji, N., and Taira, R.: The JRA-25 Reanalysis, *J. Meteor. Soc. Japan*, 85, 369–432, 2007.
- 25 Ordóñez, C., Brunner, D., Staehelin, J., Hadjinicolaou, P., Pyle, J. A., Jonas, M., Wernli, H., and Prévôt, A. S. H.: Strong influence of lowermost stratospheric ozone on lower tropospheric background ozone changes over Europe, *Geophys. Res. Lett.*, 34, L07805, doi:10.1029/2006GL029113, 2007.
- 30 Pielke, R. A., Cotton, W. R., Walko, R. L., Tremback, C. J., Lyons, W. A., Grasso, L. D., Nicholls, M. E., Moran, M. D., Wesley, D. A., Lee, T. J., and Copeland, J. H.: A comprehensive meteorological modeling system – RAMS, *Meteorol. Atmos. Phys.*, 49, 69–91, 1992.
- Pochanart, P., Hirokawa, J., Kajii, Y., Akimoto, H., and Nakao, M.: Influence of regional-scale

**Influence of
meteorological
variability on
interannual variations**

J. Kurokawa et al.

[Title Page](#)[Abstract](#)[Introduction](#)[Conclusions](#)[References](#)[Tables](#)[Figures](#)[⏪](#)[⏩](#)[◀](#)[▶](#)[Back](#)[Close](#)[Full Screen / Esc](#)[Printer-friendly Version](#)[Interactive Discussion](#)

anthropogenic activity in northeast Asia on seasonal variations of surface ozone and carbon monoxide observed at Oki, Japan, *J. Geophys. Res.*, 104(D3), 3621–3631, 1999.

Schell, B., Ackermann, I. J., Hass, H., Binkowski, F. S., and Ebel, A.: Modeling the formation of secondary organic aerosol within a comprehensive air quality model system, *J. Geophys. Res.*, 106(D22), 28275–28293, 2001.

Serreze, M. C.: Climatological aspects of cyclone development and decay in the Arctic, *Atmos.-Ocean*, 33, 1–23, 1995.

Serreze, M. C., Carse, F., and Barry, R. G.: Icelandic low cyclone activity: Climatological features, linkages with the NAO, and relationships with recent changes in the northern hemisphere circulation, *J. Climate*, 10(3), 453–464, 1997.

Streets, D. G., Bond, T. C., Carmichael, G. R., Fernandes, S. D., Fu, Q., He, D., Klimont, Z., Nelson, S. M., Tsai, N. Y., Wang, M. Q., Woo, J.-H., and Yarber, K. F.: An inventory of gaseous and primary aerosol emission in Asia in the year 2000, *J. Geophys. Res.*, 108(D21), 8809, doi:10.1029/2002JD003093, 2003.

Sudo, K., Takahashi, M., Kurokawa, J., and Akimoto, H.: CHASER: A global chemical model of the troposphere: 1. Model description, *J. Geophys. Res.*, 107(D17), 4339, doi:10.1029/2001JD001113, 2002.

Tanimoto, H., Sawa, Y., Matsueda, H., Uno, I., Ohara, T., Yamaji, K., Kurokawa, J., and Yone-mura, S.: Significant latitudinal gradient in the surface ozone spring maximum over East Asia, *Geophys. Res. Lett.*, 32, L21805, doi:10.1029/2005GL023514, 2005.

Terao, Y., Logan, J. A., Douglass, A. R., and Stolarski, R. S.: Contribution of stratospheric ozone to the interannual variability of tropospheric ozone in the northern extratropics, *J. Geophys. Res.*, 113, D18309, doi:10.1029/2008JD009854, 2008.

United Nations: Statistical Yearbook, issue 49, New York, 2005.

United Nations: Statistical Yearbook, issue 50, New York, 2006.

Uno, I., Ohara, T., Sugata, S., Kurokawa, J., Furuhashi, N., Yamaji, K., Tanimoto, N., Yumimoto, K., and Uematsu, M.: Development of the RAMS/CMAQ Asian Scale Chemical Transport Modeling System (in Japanese), *J. Jpn. Soc. Atmos. Environ.*, 40, 148–164, 2005.

Wang, X. and Mauzerall, D. L.: Characterizing distributions of surface ozone and its impact on grain production in China, Japan and South Korea: 1990 and 2020, *Atmos. Environ.*, 38, 4383–4402, 2004.

Wessel, P. and Smith, W. H. F.: New, improved version of generic mapping tools released, *EOS Trans. Amer. Geophys. Union*, 79(47), 579, 1998.

- Yamaji, K., Ohara, T., Uno, I., Tanimoto, H., Kurokawa, J., and Akimoto, H.: Analysis of the seasonal variation of ozone in the boundary layer in East Asia using the Community Multi-scale Air Quality model: What controls surface ozone levels over Japan? *Atmos. Environ.*, 40, 1856–1868, 2006.
- 5 Yamaji, K., Ohara, T., Uno, I., Kurokawa, J., Pochanart, P., and Akimoto, H.: Future prediction of surface ozone over east Asia using Models-3 Community Multiscale Air Quality Modeling System and Regional Emission Inventory in Asia, *J. Geophys. Res.*, 113, D08306, doi:10.1029/2007JD008663, 2008.
- 10 Zhang, M. G., Xu, Y., Uno, I., and Akimoto, H.: A numerical study of tropospheric ozone in the springtime in East Asia, *Adv. Atmos. Sci.*, 21(2), 163–170, 2004.

Influence of meteorological variability on interannual variations

J. Kurokawa et al.

Title Page

Abstract

Introduction

Conclusions

References

Tables

Figures

◀

▶

◀

▶

Back

Close

Full Screen / Esc

Printer-friendly Version

Interactive Discussion

Influence of meteorological variability on interannual variations

J. Kurokawa et al.

Title Page

Abstract

Introduction

Conclusions

References

Tables

Figures

⏪

⏩

◀

▶

Back

Close

Full Screen / Esc

Printer-friendly Version

Interactive Discussion



Table 1. Abbreviations used in the text.

Word	Abbreviation
ASPA	Area-weighted surface pressure anomaly (see Sect. 3.3)
BL	Boundary layer
CEC	Central eastern China
$E_{yy}M_{yy}$	The simulation using emission data sets and meteorological fields for each year
$E_{00}M_{yy}$	The simulation using the fixed emissions for 2000 and meteorological fields for each year
FA_{SJ}	Flux anomalies of springtime BL O_3 along L_{SJ}
FA_{SC}	Flux anomalies of springtime BL O_3 along L_{SC}
FA_{WJ}	Flux anomalies of springtime BL O_3 along L_{WJ}
IAV	Interannual variation
L_{SJ}	Southern boundary of WCJ (see Fig. 1)
L_{SC}	Southern boundary of CEC (see Fig. 1)
L_{WJ}	Western boundary of WCJ (see Fig. 1)
WCJ	Western and central Japan

Influence of meteorological variability on interannual variations

J. Kurokawa et al.

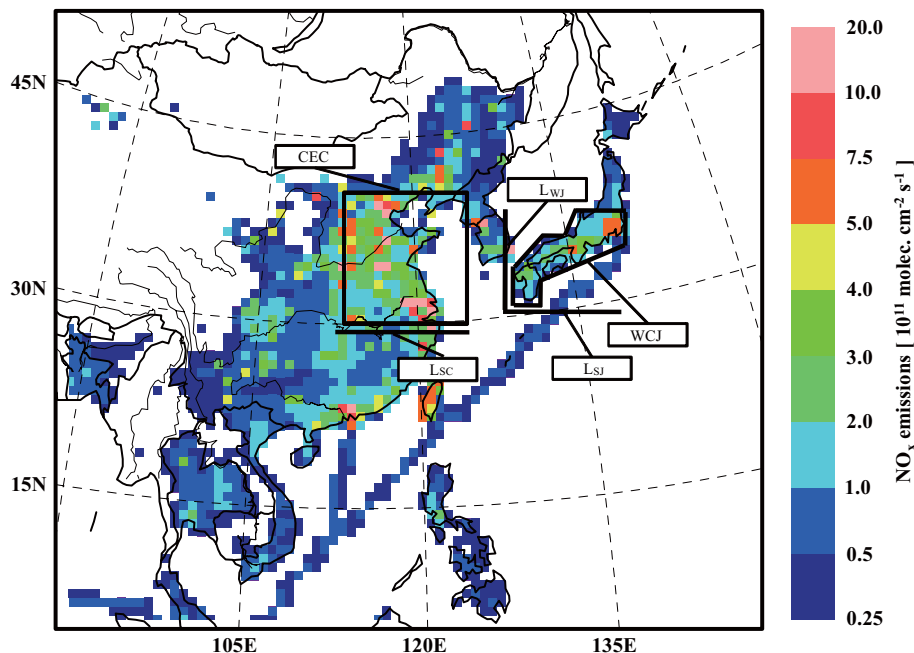


Fig. 1. Model domain of CMAQ showing the horizontal distribution of REAS NO_x emissions for 2005. The box labeled WCJ denotes western and central Japan, the focal area of our analysis of the IAV of springtime BL O_3 . The lines L_{WJ} and L_{SJ} are, respectively defined as the western and southern boundaries of WCJ, along which we calculated the BL O_3 fluxes. The box labeled CEC denotes central eastern China, and line L_{SC} is defined as the southern boundary of CEC for the calculation of BL O_3 fluxes.

[Title Page](#)[Abstract](#)[Introduction](#)[Conclusions](#)[References](#)[Tables](#)[Figures](#)[⏪](#)[⏩](#)[◀](#)[▶](#)[Back](#)[Close](#)[Full Screen / Esc](#)[Printer-friendly Version](#)[Interactive Discussion](#)

Influence of meteorological variability on interannual variations

J. Kurokawa et al.

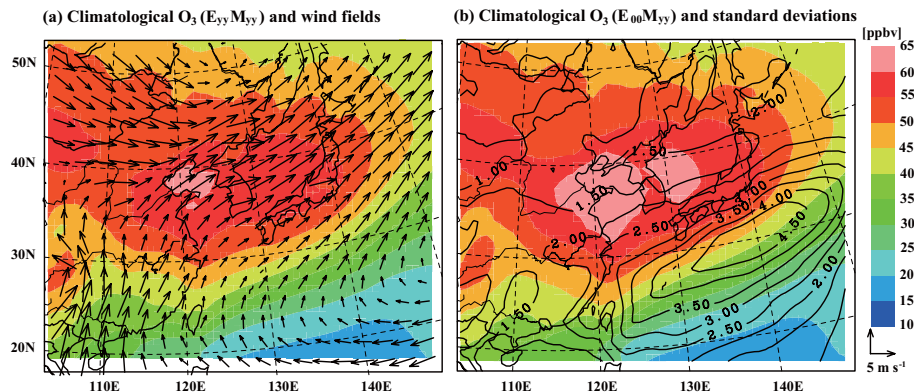


Fig. 2. (a) Spatial distributions of simulated springtime BL O₃ concentrations averaged over 1981–2005 for the $E_{yy}M_{yy}$ scenario, overlaid with springtime wind fields in the BL. (b) The same as in (a) for the $E_{00}M_{yy}$ scenario, overlaid with the standard deviations of O₃ concentrations, calculated at each grid point using the simulated fields for each year and the 25-year average.

[Title Page](#)[Abstract](#)[Introduction](#)[Conclusions](#)[References](#)[Tables](#)[Figures](#)[◀](#)[▶](#)[◀](#)[▶](#)[Back](#)[Close](#)[Full Screen / Esc](#)[Printer-friendly Version](#)[Interactive Discussion](#)

Influence of meteorological variability on interannual variations

J. Kurokawa et al.

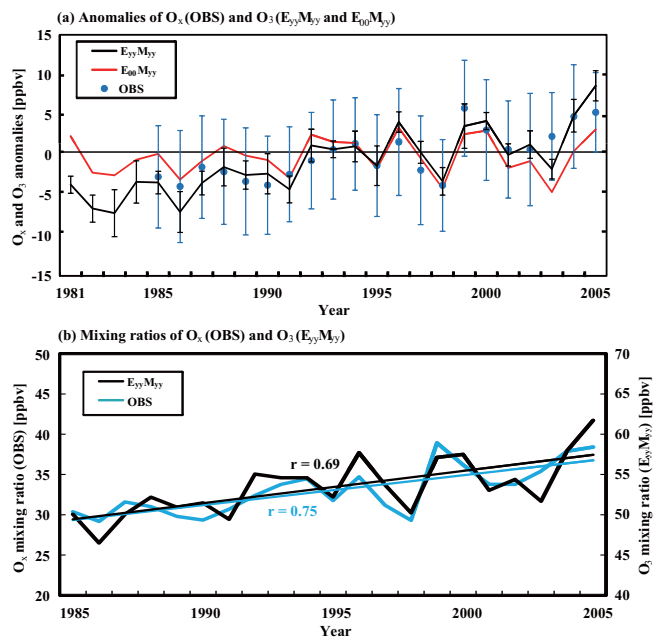


Fig. 3. (a) Time series of anomalies of springtime observed surface O_x (blue points) and simulated BL O_3 for the $E_{yy}M_{yy}$ scenario (black line) averaged over WCJ. The observational data are from air quality monitoring stations in WCJ with continuous measurements from 1985–2005. The blue whiskers indicate 1 standard deviation of observations, calculated from the springtime-averaged values at each station. The black whiskers denote the same but for the simulation based on the values of springtime BL O_3 at each grid point over WCJ. Simulated anomalies for the $E_{00}M_{yy}$ scenario (red line) are also presented. Anomalies are defined as deviations from values averaged over 1985–2005. (b) Time series of springtime surface mixing ratio of observed O_x and simulated O_3 for the $E_{yy}M_{yy}$ scenario averaged over WCJ. The blue regression line is for observation, and the black one is for simulation. Note that left and right axes are assigned for observed and simulated data, respectively.

Title Page

Abstract

Introduction

Conclusions

References

Tables

Figures

◀

▶

◀

▶

Back

Close

Full Screen / Esc

Printer-friendly Version

Interactive Discussion

Influence of meteorological variability on interannual variations

J. Kurokawa et al.

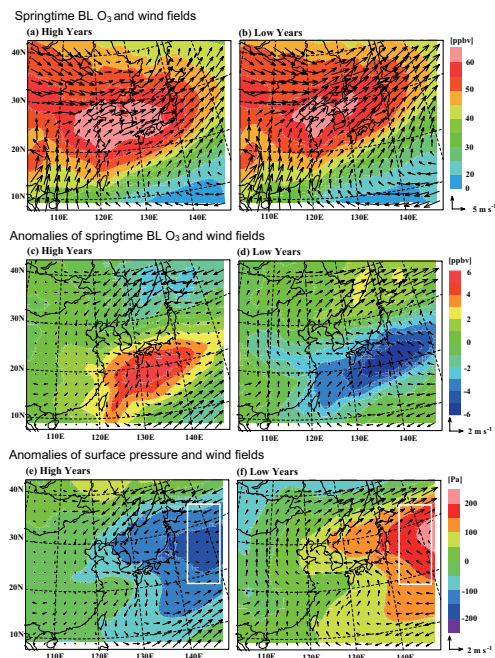


Fig. 4. Composite spatial distributions of **(a)** the springtime BL O₃ concentrations, **(c)** its anomalies, and **(e)** surface pressure anomalies during the high O₃ over WCJ years (High Years). The same information but during the low O₃ over WCJ years (Low Years) is shown in **(b)**, **(d)**, and **(f)**, respectively. Vectors in (a) and (b) indicate the composite springtime wind fields in the BL and those in (c), (d), (e), and (f) are the wind anomalies. High (low) O₃ over WCJ years were defined as the top (bottom) 5 years with respect to the springtime BL O₃ anomalies over WCJ between 1981 and 2005. The white box in (e) and (f) shows the area where the area-weighted surface pressure anomaly (ASPAs) was calculated. The $E_{00}M_{yy}$ scenario was used for the model simulation. Anomalies are defined as deviations from averaged values during 1981–2005.

Title Page

Abstract

Introduction

Conclusions

References

Tables

Figures

◀

▶

◀

▶

Back

Close

Full Screen / Esc

Printer-friendly Version

Interactive Discussion

Influence of meteorological variability on interannual variations

J. Kurokawa et al.

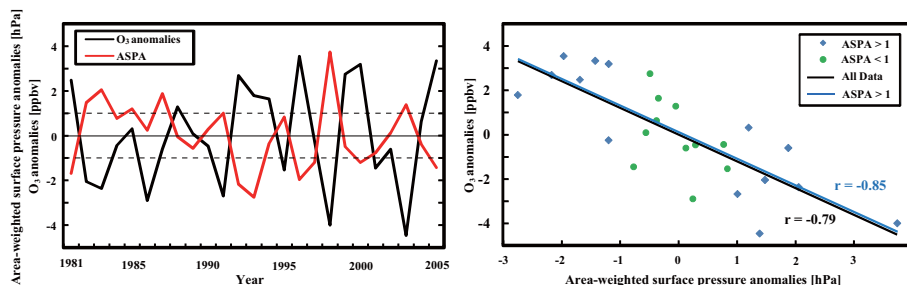


Fig. 5. Time series (left) and scatter plots (right) of springtime BL O₃ anomalies and ASPA during 1981–2005. Dashed lines indicate ± 1 hPa of ASPA. Blue and green points, respectively represent absolute values of ASPA larger (large ASPA data; 14 data points) and smaller (11 data points) than 1 hPa. The black regression line is for all data (25 data points), and the blue one is for large ASPA data. The simulation scenario and the definition of anomalies are the same as in Fig. 4.

Title Page

Abstract

Introduction

Conclusions

References

Tables

Figures

◀

▶

◀

▶

Back

Close

Full Screen / Esc

Printer-friendly Version

Interactive Discussion

Influence of meteorological variability on interannual variations

J. Kurokawa et al.

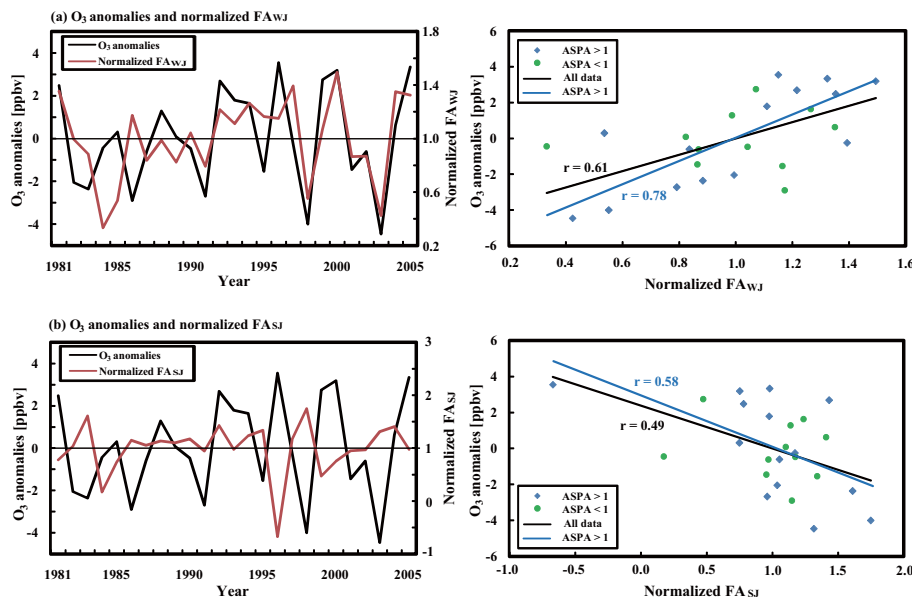


Fig. 6. (a) Time series (left) and scatter plots (right) of O_3 anomalies over WCJ and O_3 flux anomalies across the section along L_{WJ} (FA_{WJ}) in the springtime BL between 1981 and 2005. (b) The same as in (a) but with O_3 flux anomalies across the section along L_{SJ} (FA_{SJ}). See Fig. 1 for the definition of L_{WJ} and L_{SJ} . Values of FA_{WJ} and FA_{SJ} are normalized relative to the respective 25-year average. The colors of points and lines are the same as in Fig. 5. The simulation scenario and the definition of anomalies are the same as in Fig. 4.

Title Page

Abstract

Introduction

Conclusions

References

Tables

Figures

◀

▶

◀

▶

Back

Close

Full Screen / Esc

Printer-friendly Version

Interactive Discussion

Influence of meteorological variability on interannual variations

J. Kurokawa et al.

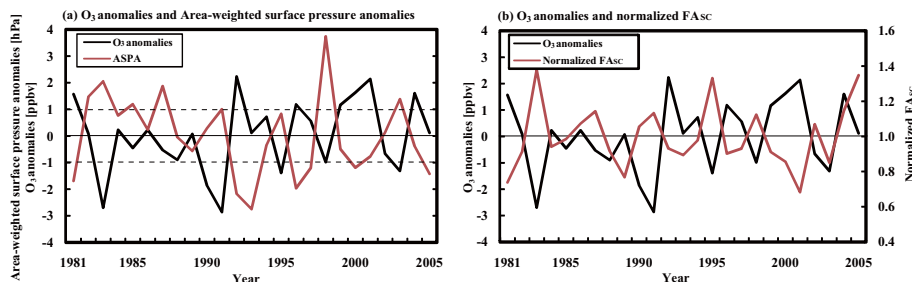


Fig. 7. (a) Time series of springtime BL O₃ anomalies over CEC and ASPA between 1981 and 2005. (b) The same as in (a) but with springtime BL O₃ flux anomalies across the section along L_{SC} (FA_{SC}). See Fig. 1 for the definition of L_{SC} . Values of FA_{SC} are normalized relative to the 25-year average. The simulation scenario and the definition of anomalies are the same as in Fig. 4.

Title Page

Abstract

Introduction

Conclusions

References

Tables

Figures

◀

▶

◀

▶

Back

Close

Full Screen / Esc

Printer-friendly Version

Interactive Discussion

Influence of meteorological variability on interannual variations

J. Kurokawa et al.

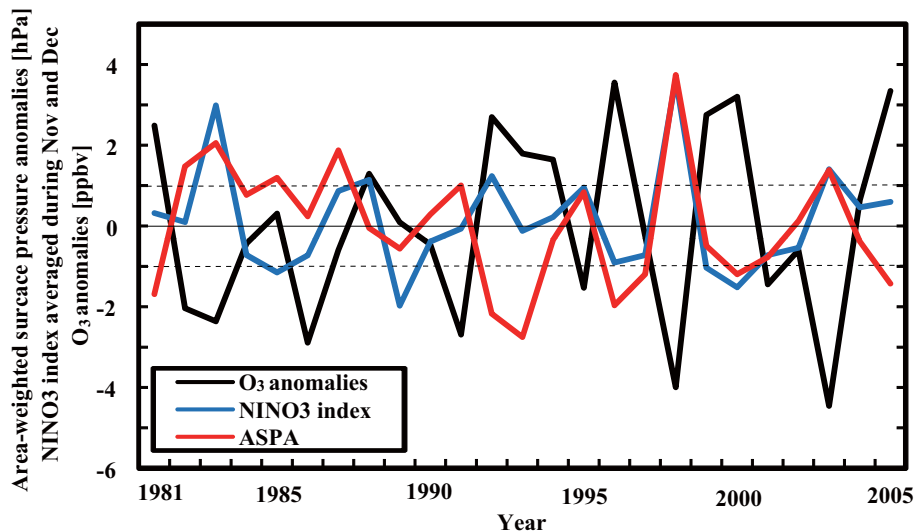


Fig. 8. Time series of springtime BL O₃ anomalies over WCJ, ASPA, and the NINO3 index averaged during November and December of the previous year. Dashed lines indicate ± 1 hPa of ASPA. The simulation scenario and the definition of anomalies are the same as in Fig. 4.

[Title Page](#)[Abstract](#)[Introduction](#)[Conclusions](#)[References](#)[Tables](#)[Figures](#)[◀](#)[▶](#)[◀](#)[▶](#)[Back](#)[Close](#)[Full Screen / Esc](#)[Printer-friendly Version](#)[Interactive Discussion](#)

Influence of meteorological variability on interannual variations

J. Kurokawa et al.

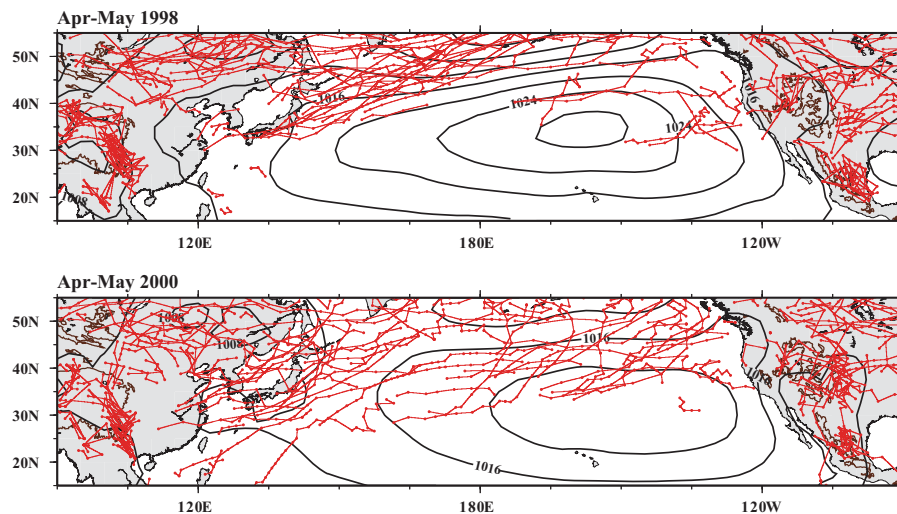


Fig. 9. Spatial distributions of mean sea level pressure overlaid with cyclone tracks during April and May 1998 (top, El Niño) and 2000 (bottom, La Niña).

[Title Page](#)[Abstract](#)[Introduction](#)[Conclusions](#)[References](#)[Tables](#)[Figures](#)[◀](#)[▶](#)[◀](#)[▶](#)[Back](#)[Close](#)[Full Screen / Esc](#)[Printer-friendly Version](#)[Interactive Discussion](#)